Journal of Physics: Conference Series **1596** (2020) 012053 doi:10.1088/1742-6596/1596/1/012053

Cerenkov-free RIP Maxwell solver: dispersionless along X

Alexander Pukhov

Institut fuer Theoretische Physik I, Universitaet Duesseldorf, 40225 Germany

E-mail: pukhov@tp1.hhu.de

Abstract. A semi-implicit finite-difference time-domain (FDTD) numerical Maxwell solver is presented for full electromagnetic Particle-in-Cell (PIC) codes for the simulations of plasma-based acceleration. The solver projects the volumetric Yee lattice into planes transverse to a selected axis (the particle acceleration direction) that makes the scheme quasi-one-dimensional. The fields positions build rhombi in plane (RIP) patterns. The RIP scheme uses a compact local stencil that makes it perfectly suitable for massively parallel processing via domain decomposition along all three dimensions. No global/local spectral methods are involved. The scheme removes the numerical dispersion of electromagnetic waves running parallel to the selected axis. The scheme shows no numerical Cerenkov instability (NCI).

1. Introduction

Plasma-based particle acceleration is a rapidly developing route towards future compact accelerators [1, 2, 3, 4]. The reason is that plasmas support fields orders of magnitude higher than in conventional accelerators [5, 6]. Thus, particle acceleration can be accomplished on much shorter distances as compared with the solid-state accelerating structures. However, the plasma is a highly nonlinear medium and requires accurate and computationally efficient numerical modeling to understand and tune the acceleration process. The main workhorse for plasma simulations are Particle-in-Cell codes [7, 8, 9, 10, 11]. These provide the most appropriate description of plasma as an ensemble of particles pushed according to the relativistic equations of motion using self-consistent electromagnetic fields, which are maintaned on a spatial grid [12].

We here consider full electromagnetic (EM) PIC codes which are usually applied for Laser Wake Field Acceleration (LWFA) in plasmas. The full EM PIC correctly describes the laser evolution even in highly nonlinear regimes.

Most of the FDTD Maxwell solvers used in EM PIC codes employ the staggered Yee lattice [13]: individual components of the electromagnetc fields are located at staggered positions in space and time. The resulting numerical scheme includes a Courant stability restriction on the time step which leads to numerical dispersion. This results in electromagnetic waves with phase velocities below the vacuum speed of light. Thus, the relativistic particles may stay in resonance with the waves and radiate . This non-physical Cerenkov radiation plagues the Lorentz-boosted PIC simulations [14]. Moreover, even normal PIC simulations in the laboratory frame suffer from the numerical Cerenkov effect [15, 16]. Any high-density bunch of relativistic particles - e.g. the accelerated witness bunch - emits Cerenkov radiation as well. This affects the bunch energy and emittance [17].

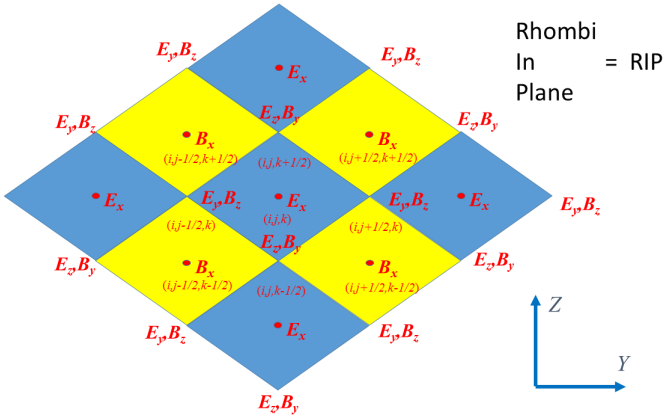

Figure 1. The "rhombi-in-plane" RIP grid.

We conclude, the Yee lattice is not optimal for simulating high energy applications and a better FDTD scheme is required that removes the numerical dispersion.

2. The general quasi-1D Maxwell solver

We here present a FDTD 3D Maxwell solver that has no numerical dispersion for plane waves propagating in one selected direction. In plasma-based acceleration this is usually the direction of particle acceleration: the driving laser optical axis. The solver should retain its dispersionless properties not only in vacuum, but also inside dense plasmas, i.e. the optimal time step/grid step relation should not be compromised by the presence of plasma. The solver must not use spectral transformations and should have a compact local stencil. This is the pre-requisite for efficient parallelization via domain decomposition. In short, we develop an efficient Maxwell solver for quasi-1D problems.

We select the $X-$direction for dispersionless propagation. We use a semi-implicit trapezoidal scheme for the discretization of the transverse fields on a 3D grid. We write here explicitly the $i-$index along the $X-$axis only as the scheme can be easily generalized for arbitrary transverse geometries (e.g. Cartesian, or cylindrical, etc.):

$$\frac{E^{n+1}_{y(i+1)}+E^{n+1}_{y(i)}-E^{n}_{y(i+1)}-E^{n}_{y(i)}}{2c\tau} = -\frac{-B^{n+1}_{z(i)}+B^{n+1}_{z(i+1)}-B^{n}_{z(i)}+B^{n}_{z(i+1)}}{2h_x}+\Gamma^{n+1/2}_{y(i+1/2)} \quad (1)$$

$$\frac{E^{n+1}_{z(i+1)}+E^{n+1}_{z(i)}-E^{n}_{z(i+1)}-E^{n}_{z(i)}}{2c\tau} = \frac{-B^{n+1}_{y(i)}+B^{n+1}_{y(i+1)}-B^{n}_{y(i)}+B^{n}_{y(i+1)}}{2h_x}+\Gamma^{n+1/2}_{z(i+1/2)} \quad (2)$$

$$\frac{E^{n+1}_{x(i)}-E^{n}_{x(i)}}{c\tau} = \Gamma^{n+1/2}_{x(i)} \quad (3)$$

$$\frac{B^{n+1}_{y(i)}+B^{n+1}_{y(i+1)}-B^{n}_{y(i)}-B^{n}_{y(i+1)}}{2c\tau} = \frac{-E^{n+1}_{z(i)}+E^{n+1}_{z(i+1)}-E^{n}_{z(i)}+E^{n}_{z(i+1)}}{2h_x}+\Phi^{n+1/2}_{y(i+1/2)} \quad (4)$$

$$\frac{B^{n+1}_{z(i)}+B^{n+1}_{z(i+1)}-B^{n}_{z(i)}-B^{n}_{z(i+1)}}{2c\tau} = -\frac{-E^{n+1}_{y(i)}+E^{n+1}_{y(i+1)}-E^{n}_{y(i)}+E^{n}_{y(i+1)}}{2h_x}+\Phi^{n+1/2}_{z(i+1/2)} \quad (5)$$

$$\frac{B^{n+1}_{x(i)}-B^{n}_{x(i)}}{c\tau} = \Phi^{n+1/2}_{x(i)} \quad (6)$$

Here, τ is the time step and h_x is the spatial grid step in the $X-$direction.

These equations (1)-(6) build a system of coupled linear equations relating the updated fields at the time step $n+1$ with already known fields at the time steps n and $n+1/2$. Although this implicit system of linear equations can generally be solved using a fast matrix inversion method (the system has a sparse matrix), we will be interested in the **special case** $c\tau = h_x = \Delta$. In this particular case, the inversion is straightforward.

First, we add/subtract Eqs. (1)+(5) and (2)+(4). to obtain transport components or simply

$$T^{+(n+1)}_{y(i)} = E^{n+1}_{y(i)} + B^{n+1}_{z(i)} = T^{+(n)}_{y(i-1)} + \Delta\left(\Gamma^{n+1/2}_{y(i-1/2)} + \Phi^{n+1/2}_{z(i-1/2)}\right) \quad (7)$$

$$T^{+(n+1)}_{z(i)} = E^{n+1}_{z(i)} + B^{n+1}_{y(i)} = T^{+(n)}_{z(i+1)} + \Delta\left(\Gamma^{n+1/2}_{z(i+1/2)} + \Phi^{n+1/2}_{y(i+1/2)}\right) \quad (8)$$

and

$$T^{-(n+1)}_{y(i)} = E^{n+1}_{y(i)} - B^{n+1}_{z(i)} = T^{-(n)}_{y(i+1)} + \Delta\left(\Gamma^{n+1/2}_{y(i+1/2)} - \Phi^{n+1/2}_{z(i+1/2)}\right) \quad (9)$$

$$T^{-(n+1)}_{z(i)} = E^{n+1}_{z(i)} - B^{n+1}_{y(i)} = T^{-(n)}_{z(i-1)} + \Delta\left(\Gamma^{n+1/2}_{z(i-1/2)} - \Phi^{n+1/2}_{y(i-1/2)}\right) \quad (10)$$

These are the marching equations. The transport components $T^{+/-}_{y,z}$ must be shifted one cell in the corresponding direction and the diffraction/refraction terms be correctly added.

3. The three-dimensional RIP Maxwell solver in Cartesian coordinates

Let us now look at the diffraction/refraction terms. For simplicity, we use Cartesian coordinates.

We project the Yee lattice onto the (Y, Z) plane. The grid becomes planar and has the form of Rhombi-in-Plane (RIP), as shown in Fig. 1. The pairs of transverse fields are now combined at positions according to the transport properties (7)-(10). The pair $\mathbf{E_y}, \mathbf{B_z}$ is located at the rhombi vertices $(i, j+1/2, k)$. The pair $\mathbf{E_z}, \mathbf{B_y}$ is located at the rhombi vertices $(i, j, k+1/2)$. The longitudinal field $\mathbf{E_x}$ we place at point (i, j, k) which is the center of the full integer rhombus. The longitudinal field $\mathbf{B_x}$ we place at the center of the half integer rhombus $(i, j+1/2, k+1/2)$. The grid is shown in Fig.1.

Then, the diffraction/refraction terms at the half time step will be:

$$\Gamma^{n+1/2}_{y(i+1/2,j+1/2,k)} = \left(\frac{\partial B_x}{\partial z} - j_y\right)|^{n+1/2}_{i+1/2,j+1/2,k} = -\frac{1}{2}\left(j^{n+1/2}_{y,(i,j+1/2,k)} + j^{n+1/2}_{y,(i+1,j+1/2,k)}\right) + \quad (11)$$
$$+ \frac{B^{n+1/2}_{x(i,,j+1/2,k+1/2)} + B^{n+1/2}_{x(i+1,,j+1/2,k+1/2)} - B^{n+1/2}_{x(i,j+1/2,k-1/2)} - B^{n+1/2}_{x(i+1,j+1/2,k-1/2)}}{2h_z}$$

$$\Gamma^{n+1/2}_{z(i+1/2,j,k+1/2)} = \left(-\frac{\partial B_x}{\partial y} - j_y\right)|^{n+1/2}_{i+1/2,j,k+1/2} = -\frac{1}{2}\left(j^{n+1/2}_{z,(i,j,k+1/2)} + j^{n+1/2}_{z,(i+1,j,k+1/2)}\right) - \quad (12)$$
$$- \frac{B^{n+1/2}_{x(i,,j+1/2,k+1/2)} + B^{n+1/2}_{x(i+1,j+1/2,k+1/2)} - B^{n+1/2}_{x(i,j-1/2,k+1/2)} - B^{n+1/2}_{x(i+1,j-1/2,k+1/2)}}{2h_y}$$

$$\Gamma^{n+1/2}_{x(i,j,k)} = \left(\frac{\partial B_z}{\partial y} - \frac{\partial B_y}{\partial z} + j_x\right)|^{n+1/2}_{i,j,k} = -j^{n+1/2}_{x,(i,j,k)} \quad (13)$$
$$+ \frac{B^{n+1/2}_{z(i,,j+1/2,k)} - B^{n+1/2}_{z(i,,j-1/2,k)}}{h_y} - \frac{B^{n+1/2}_{y(i,,j,k+1/2)} - B^{n+1/2}_{y(i,,j,k-1/2)}}{h_z}$$

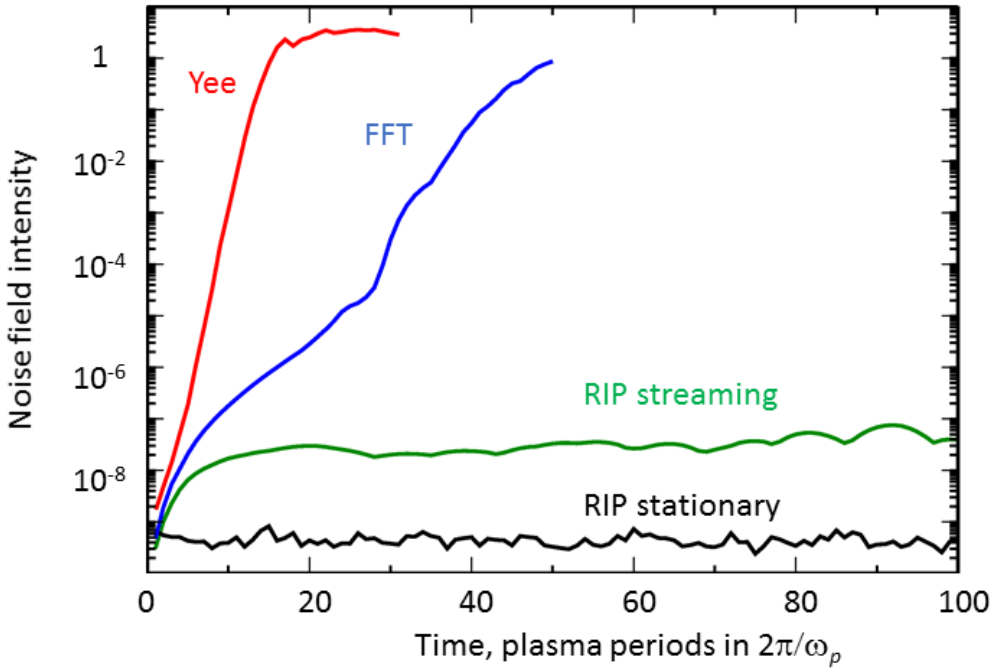

Figure 2. Intensity of NCI-caused fluctuating fields in the "streaming plasma" simulations for various Maxwell solvers.

$$\Phi^{n+1/2}_{y(i+1/2,j,k+1/2)} = -\frac{E^{n+1/2}_{x(i,,j,k+1)} + E^{n+1/2}_{x(i+1,,j,k+1)} - E^{n+1/2}_{x(i,j,k)} - E^{n+1/2}_{x(i+1,j,k)}}{2h_z} \tag{14}$$

$$\Phi^{n+1/2}_{z(i+1/2,j+1/2,k)} = \frac{E^{n+1/2}_{x(i,,j+1,k)} + E^{n+1/2}_{x(i+1,,j+1,k)} - E^{n+1/2}_{x(i,j,k)} - E^{n+1/2}_{x(i+1,j,k)}}{2h_y} \tag{15}$$

$$\Phi^{n+1/2}_{x(i,j+1/2,k+1/2)} = -\left(\frac{\partial E_z}{\partial y} - \frac{\partial E_y}{\partial z}\right)|^{n+1/2}_{i,j+1/2,k+1/2} = \tag{16}$$

$$- \frac{E^{n+1/2}_{z(i,,j+1,k+1/2)} - E^{n+1/2}_{z(i,,j,k+1/2)}}{h_y} + \frac{E^{n+1/2}_{y(i,,j+1/2,k+1)} - E^{n+1/2}_{y(i,,j-1/2,k+1/2)}}{h_z}$$

Similar formulas are obtained for the fields at the half-time steps. The use of the transport vectors $\mathbf{T}_\perp$ makes the boundary conditions in the $x-$direction trivial.

It seems that we have to maintain two sets of fields for each time step: fields at the full step and at the half step. The particles however, can be pushed just once per time step. Currents at the full time step required to push the half-time step fields can be obtained by simple averaging on the grid. Finally, the RIP scheme is conservative and symplectic.

The fields at the half-time steps are required to calculate the diffraction terms only. Without diffraction, the need to maintain the additional set of fields at half-time steps vanishes and the RIP scheme becomes identical to the standard 1D PIC scheme [12], which is the workhorse of 1D plasma simulations due to its excellent stability and accuracy.

4. Dispersion and stability of the RIP scheme

We apply the plane-wave analysis to the marching equations (3), (6) with the refraction/diffraction terms (11)-(16) assuming $\mathbf{F} = \tilde{\mathbf{F}} \exp(-i\omega t + i\mathbf{kr})$. For simplicity, we assume

uniform plasma frequency $\omega_p^2 = 4\pi n e^2/\gamma$ and the linear current response to the electric field $\frac{2c}{\Delta}\sin\frac{\omega\tau}{2}\tilde{\mathbf{J}} = iq^2 n\tilde{\mathbf{E}}$. For the case of interest, $c\tau = h_x = \Delta$, the stability condition in In the presence of plasmas is

$$\frac{1}{\Delta^2} > \frac{1}{h_y^2} + \frac{1}{h_z^2} + \frac{c^2\omega_p^2}{4} \tag{17}$$

The RIP scheme combines dispersionless properties of the standard 1D solver along the $X-$axis with the Yee dispersion for waves running in the transverse direction. Indeed, setting $k_y = k_z = 0$ in the dispersion relation, we immediately obtain $\omega = ck_x$ and the phase velocity

$$V_{ph} = \frac{\omega}{k_x} = c \tag{18}$$

for plane waves propagating in the $X-$direction.

5. Numerical Cerenkov instability test

As a numerical test, we take the numerical Cerenkov instability. We compare the standard Yee solver, an FFT-based solver and the RIP solver, all implemented on the VLPL platform [8]. No artificial filtering of fields or currents is used. The initial configuration is a spherical plasma of Gaussian density profile $n = n_0\exp\left(-r^2/\sigma^2\right)$ consisting of electrons and protons moving in the $X-$direction with the average momentum $< \mathbf{p_0} > /m_\alpha c = (p_{x0}, 0, 0)$, where α denotes the particle type ($\alpha = e, p$), with $m_p/m_e = 1846$. To seed the instability, the electrons have a small initial temperature $< (\mathbf{p}_0 - < \mathbf{p}_0 >)^2 >= \sigma_p^2$. In relativistically normalized units, the simulation parameters are: the peak plasma density is $n_0 = 1$ with the corresponding non-relativistic plasma frequency $\omega_p = \sqrt{4\pi n_0 e^2/m_e}$. The initial particle momenta are $p_{x0} = -10$ and $\sigma_p = 10^{-4}$. The grid steps were $h_y = h_z = 1.88\, c/\omega_p$ and $h_x = c\tau = \Delta = 0.63\, c/\omega_p$. As a diagnostics for the comparison, we selected the growth of the maximum local field intensity $I = \mathbf{E^2} + \mathbf{B}^2$ on the grid. The results are shown in Fig.2

We see that the fluctuating fields in simulations using the Yee scheme grow to the non-linear saturation within a few plasma oscillations. This is because the Yee solver is exposed to the first order Cerenkov resonance. The FFT-based solver is dispersionless and avoids the first order Cerenkov resonance. Still, the second order aliasing of the spectral FFT solver leads to the numerical Cerenkov instabilty, though at a lower growth rate as compared with the standard Yee solver.

In contrast, the RIP solver is apparently free from NCI. The noise in the RIP scheme remains many orders of magnitude lower over a long simulation time of $t = 100 \cdot 2\pi/\omega_p$. The very slow growth of the noise fields here has nothing to do with the Cerenkov resonance, but is the unavoidable "numerical heating" always present in PIC codes.

We mention here that the numerical Cerenkov instability of uniformly streaming plasma can be alleviated by using a co-moving grid as proposed by Lehe et al. [18]. The method exploits a Galilean transformation to a grid in which the background plasma does not stream through the cell boundaries. Yet, when a dense bunch of accelerated particles moves in the oppisite direction at twice the light speed relative to this grid and is fully exposed to the Cerenkov resonance.

The RIP scheme does not shift the numerical grid with the relativistic plasma particles. Rather, it shifts the electromagnetic field components exactly by one grid cell at each time step, see Eqs. (7)-(10). Most probably, this is the reason for the extremely low level of NCI in the RIP Maxwell solver even at the aliased modes.

6. Discussion

The new RIP scheme is a compact stencil FDTD Maxwell solver that removes the numerical dipersion in one selected direction. For the waves propagating in the transverse direction,

it corresponds to the Yee solver. The RIP scheme is local and does not use any global spectral method. This allows for efficient parallelization via domain decomposition in all three dimensions. The computational costs of the RIP solver is comparable with that of the Yee solver. The RIP solver can be used for simulations of quasi-1D physics problems like laser wake field acceleration.

Acknowledgements
This work has been supported in parts by BMBF and DFG (Germany).

References

[1] ALEGRO Collaboration, "Towards an Advanced Linear International Collider" arXiv:1901.10370 (2019)
[2] W. Leemans and E. Esarey, "Laser-driven plasma-wave electron accelerators" Physics Today **62**, 3, 44 (2009)
[3] http://eupraxia-project.eu
[4] C. Joshi and A. Caldwell, "Plasma Accelerators", in Accelerators and Colliders, edited by S. Myers and H. Schopper (Springer Berlin Heidelberg, Berlin, Heidelberg, 2013), Chap. 12.1, pp. 592 – 605.
[5] T. Tajima and J. M. Dawson. Phys. Rev. Lett. **43**, 267 (1979)
[6] E. Esarey, C. B. Schroeder, W. P. Leemans, Rev. Mod. Phys. **81**, 1229 (2009).
[7] Fonseca RA, Martins SF, Silva LO, Tonge JW, Tsung FS, Mori WB, "One-to-one direct modeling of experiments and astrophysical scenarios: pushing the envelope on kinetic plasma simulations", Plasma Physics and Controlled Fusion vol. **50**, 124034 (2008)
[8] A. Pukhov, "Particle-In-Cell Codes for Plasma-based Particle Acceleration", CERN Yellow Rep. 1 , 181 (2016).
[9] T. D. Arber, K. Bennett, C. S. Brady, A. Lawrence-Douglas, M. G. Ramsay, N. J. Sircombe, P. Gillies, R. G. Evans, H. Schmitz, A. R. Bell and C. P. Ridgers. "Contemporary particle-in-cell approach to laser-plasma modelling", Plasma Phys. Control. Fusion **57**, 113001 (2015).
[10] Jean-Luc Vay, Irving Haber, Brendan B. Godfrey, "A domain decomposition method for pseudo-spectral electromagnetic simulations of plasmas", Journal of Computational Physics **243**, 260 (2013).
[11] J. Derouillat, A. Beck, F. Perez, T. Vinci, M. Chiaramello, A. Grassi, M. Fl , G. Bouchard, I. Plotnikov, N. Aunai, J. Dargent, C. Riconda, M. Grech, SMILEI: a collaborative, open-source, multi-purpose particle-in-cell code for plasma simulation, Comput. Phys. Commun. **222**, 351-373 (2018)
[12] C.K. Birdsall and A.B. Langdon, Plasma Physics via Computer Simulations (Adam Hilger, New York, 1991). http://dx.doi.org/10.1887/0750301171
[13] Yee K S "Numerical solution of initial boundary value problems involving maxwell's equations in isotropic media" 1966 IEEE Trans. Antennas Propag. 14 302–7
[14] J.-L. Vay, C.G.R. Geddes, E. Cormier-Michel, D.P. Grote "Numerical methods for instability mitigation in the modeling of laser wakefield accelerators in a Lorentz-boosted frame" Journal of Computational Physics **230** (2011) 5908–5929.
[15] D.-Y. Na , J. L. Nicolini , R. Lee , B.-H. V. Borges , Y. A. Omelchenko , F. L. Teixeira "Diagnosing numerical Cherenkov instabilities in relativistic plasma simulations based on general meshes" arXiv:1809.05534 (2019)
[16] R. Nuter, V. Tikhonchuk, Suppressing the numerical cherenkov radiation in the yee numerical scheme, Journal of Computational Physics **305** (2016) 664 – 676. doi:https://doi.org/10.1016/ j.jcp.2015.10.057.
[17] R. Lehe, A. Lifschitz, C. Thaury, and V. Malka "Numerical growth of emittance in simulations of laser-wakefield acceleration", PRSTAB **16**, 021301 (2013)
[18] Remi Lehe, Manuel Kirchen, Brendan B. Godfrey, Andreas R. Maier, and Jean-Luc Vay "Elimination of numerical Cherenkov instability in flowing-plasma particle-in-cell simulations by using Galilean coordinates" Phys. Rev. E 94, 053305 (2016).